

# High-Power CW-DFB LDs for Optical Communications

by Keishi Takaki\*, Tomofumi Kise\*, Kazuomi Maruyama\*, Koji Hiraiwa\*,  
Nobumitsu Yamanaka\*, Masaki Funabashi\* and Akihiko Kasukawa\*

**ABSTRACT** CW-DFB Lasers can be used for WDM and CATV applications by combining them with external modulators. For WDM application, we successfully obtained a low driving current of less than 200 mA at 40 mW from S-band to L-band by taking care of the optical confinement of the MQW structure. On the other hand, by optimizing cavity length and coupling coefficient, we achieved a high output power of 175 mW and a narrow linewidth of 0.8 MHz even at 100 mW for CATV applications.

## 1. INTRODUCTION

Wavelength Division Multiplexing (WDM) is a very effective and common system for today's heavy traffic of optical communication. Distributed Feedback Lasers (DFB-LDs), including periodical grating structures, are key devices as signal sources due to their highly selected single emission wavelengths. Table 1 shows the classified lists and the characteristics of DFB Lasers. In these DFB LDs, continuous wave (CW) DFB LDs are used for long haul applications by combining them with external modulators such as LiNbO<sub>3</sub>, and many characteristics are demanded. We list up some of them below.

- (1) Wide wavelength band (Conventional C-band and both sides of S and L-band)
- (2) Dense channel spacing (from 100 GHz to 50 GHz and 25 GHz)
- (3) High data rate (10 Gb/s and 40 Gb/s)
- (4) High output power and low driving current (up to 40 mW)
- (5) High reliability

To broaden the band, conventional C-band and both sides of S-band and L-band<sup>1)</sup> can be used to increase the number of channels. Dense channel spacing is another solution to increase the number of channels and an attempt to shift from 100 GHz to 50 GHz (twice of the number of channels) and 25 GHz (4 times) is expected<sup>2)</sup>. To achieve this, the wavelength stability is important and peripheral technologies have been developed successfully. High data rates of 10 Gb/s and 40 Gb/s have been achieved in the external modulators. Output power is increased to 40 mW in WDM, but a higher output power (over 80 mW) is demanded for a large number of ports in CATV applications<sup>4)-7)</sup>. CATV systems demand extremely low noise characteristics to keep a high signal to noise ratio (S/N ratio). To maintain a high S/N ratio after long

fiber propagation, low Relative Intensity Noise (RIN) and narrow linewidth (which shows phase noise convertible to intensity noise after fiber propagation) are key characteristics.

In this paper, we report our activities to achieve a low driving current for WDM applications. As high power technologies expand, we are also developing higher output power operation and narrow linewidth for CATV applications. In Section 2 we show the chip structures of DFB LDs and their grating fabrication technique. Optimization of coupling coefficient and cavity length to obtain a low driving current is described in Section 3. Optical confinement optimization, especially in the L-band, is described in Section 4. For expansion to CATV applications, efforts to achieve a narrow spectral linewidth are described in Section 5.

## 2. CHIP DESIGN AND FABRICATION

In this section, we describe the chip structure and the key fabrication technology. Figure 1 shows the structure of the LDs used in this experiment. These devices were 1.55  $\mu\text{m}$  InGaAsP-InP buried hetero-structure (BH) DFB LDs grown by MOCVD. The 2  $\mu\text{m}$  wide active layers of these

**Table 1** Classified lists and characteristics of DFB lasers.

Design	Modulation	Transmission Distance	Speed	Cost	Characteristic
CW	External modulator	Long-haul 100 km~	~40 Gbps (Typ.10 Gbps)	High	Long-haul Large capacity
EA	Integrated modulator	Metro ~100 km	~10 Gbps	Medium	Low-chirp Small-package
DM	Direct modulation	Metro-Access 10~100 km	~10 Gbps	Medium	Low-cost Small-package
Uncooled	Direct modulation	Access ~10 km	~10 Gbps (Typ.2.5 Gbps)	Low	Very low-cost Very small-size

\* Photonics & Packaging Technologies, Yokohama R & D Lab.

LDs were strain compensated and consist of six quantum-wells. The Far-Field Pattern (FFP) of these LDs is  $24^\circ$  (vertical) and  $20^\circ$  (horizontal), so these LDs can be easily coupled with fiber. To achieve high slope efficiency and low driving current, both facets are coated with anti-reflective (AR) and high-reflective (HR) asymmetric coatings.

The emission wavelength of DFB LD is precisely controlled by electron beam (EB) lithography and is expressed by the equation below.

$$\lambda_{Bragg} = 2d_{pitch} \times n_{eff} \quad (1)$$

Here,  $\lambda_{Bragg}$  is the emission wavelength obtained from the grating pitch,  $d_{pitch}$  is the period of the grating, and  $n_{eff}$  is the effective refraction index in the waveguide layer. The mechanical resolution of the emission wavelength in EB lithography is about 10 pm, however, the emission wavelength has inaccuracies ( $\sim 1$  nm) originating from the facet phases, so the controllability of the emission wavelength is determined by this inaccuracy. About a 240 nm grating pitch, from which an emission wavelength of 1550 nm is obtained, was patterned by dry etching the semiconductor layers.

These LDs are packaged in standard 14-pin butterfly modules, which include two lenses, an isolator and a thermoelectric cooler (TEC). Coupling efficiency to the polarization maintaining fiber (PMF) is as high as about 75 %.

### 3. HIGH POWER AND LOW DRIVING CURRENT

First, we describe our development in high power operation. The cavity length ( $L$ ) and the coupling coefficient ( $\kappa$ ) are the key design parameters for high power operation. The coupling coefficient is a characteristic parameter of DFB LDs, and it expresses the amount of optical feedback in the grating layer.  $\kappa$  can be designed from the difference between the refractivity of grating and waveguide layer, the interval from grating to active layer, and the thickness of the grating layer. Figure 2 shows the slope efficiency of the output power (SE) and the maximum output power as a function of the  $\kappa L$  product. Here, the cavity length of these LDs is fixed as  $L=400 \mu\text{m}$ . As shown in this figure, SE and the maximum output power ( $P_{max}$ ) increase as  $\kappa$

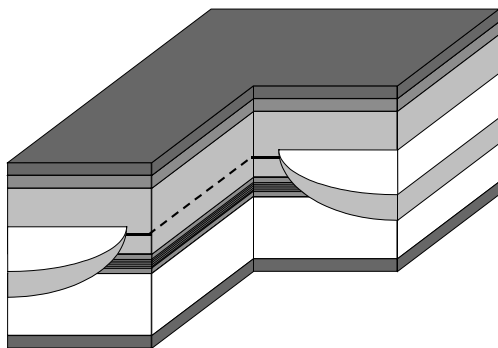


Figure 1 Schematic figure of distributed feedback laser diode (DFB LD) along longitudinal and lateral sections.

decreases. Since many characteristics such as threshold current ( $I_{th}$ ) and SE are determined by  $\kappa L$ , decreases of  $I_{th}$  and SE due to large feedback efficiency can be observed in a large  $\kappa L$ . The typical value of  $\kappa L$  product is considered to maintain a high side mode suppression ratio (SMSR), and we have to design the  $\kappa$  value for every cavity length. Power saturation seems to be mainly caused by heating around the active layers, so a large thermal conductivity, which is obtained by a long cavity, is very effective to get a higher  $P_{max}$ . In these long cavities, we have to control the  $\kappa$  to a very small value, which seems to be difficult in terms of its reproducibility. Figure 3 shows the L-I curves of these modules for different cavity lengths. In  $L=400 \mu\text{m}$ , we achieved a very high SE of 0.3 W/A and a driving current of 80 mA for a fiber coupled power ( $P_f$ ) of 20 mW. A little degradation of SE can be observed with a long cavity, but we also achieved a maximum  $P_f$  of 175 mW. This is the highest value for a commercial package including two lenses, TEC, and isolator, and is reported elsewhere<sup>8)</sup>. The spectrum of this LDM is shown in Figure 4. As shown in this figure, we can get a SMSR of more than 50 dB. Wavelength stability is considered to be another benefit of a long cavity. These results show that we achieved very high slope efficiency for every cavity length and maximum output power. Considering WDM application, the output power range is from 10 mW to 40 mW, and we can obtain the minimum driving current with a 400  $\mu\text{m}$  cavity (Table 2). On the other hand, in CATV

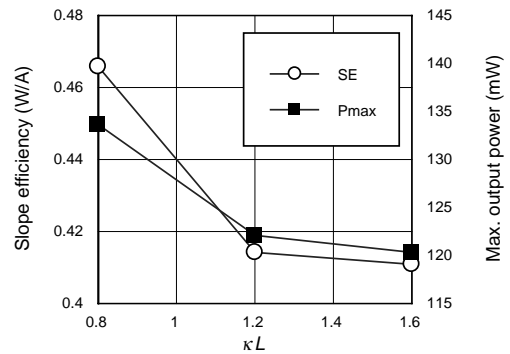


Figure 2  $\kappa L$  dependence of slope efficiency and maximum output power at  $L=400 \mu\text{m}$ .

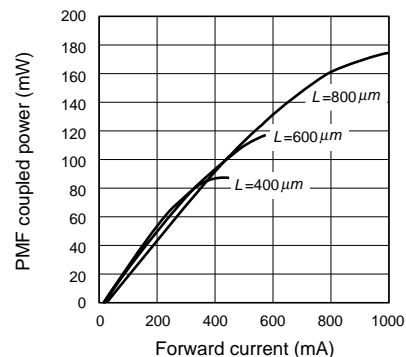
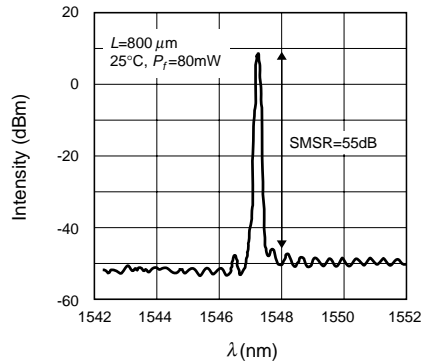


Figure 3 L-I curves of LDMs each having a different cavity length.



**Figure 4** Spectrum of the  $L=800 \mu\text{m}$  cavity at an output power of 80 mW.

**Table 2** Characteristics of LDMs with different cavity lengths.

$L$ [ $\mu\text{m}$ ]	$I_{th}$ [mA]	$Se$ [W/A]	$I_{op}$ (40 mW) [mA]	$R_{th}$ [K/W]
400	10	0.3	155	40
600	17	0.28	165	28
800	24	0.25	180	19

applications the highest output power is 175 mW for  $L=800 \mu\text{m}$ . So, we have to use an optimized cavity length considering the applications.

#### 4. S-, L-BAND DFB LDS

In this section, we describe the broadening of the wavelength band, which is the most important factor for increasing the number of channels. At present, C-band and L-band erbium-doped fiber amplifier (EDFA), having wavelength channel counts ranging from 80 to 160 per direction, are used for long-distance transmission systems. Compared to C-band, the increase of threshold current density ( $J_{th}$ ) and decrease of slope efficiency (SE) are considered to be factors that make for poor characteristics in the L-band. Besides, these factors are caused by an increase of non-radiate re-combination and a decrease of photon energy due to the variety of effective mass and energy band gap<sup>1)</sup>. We optimized electrical and optical confinement in the active region to overcome these problems. Figure 5 is a schematic figure of the MQW structure in the L-band. The barrier band gap (Figure 5 c) was decreased while the difference in the band gap between well and barrier layers was kept the same as that of the C-band. As a result, optical confinement inside the active region is increased. On the other hand, the carrier can easily flow through the barrier layer and non-uniformity of the carrier density along the vertical axis is suppressed. To investigate the characteristics inside the active region, we fabricated the broad contact lasers without grating layers. The  $J_{th}$  values in these broad contact lasers with the design shown in Figure 5 c are  $880 \text{ A/cm}^2$ , and these values are as low as those of the C-band structure ( $J_{th} \sim 850$

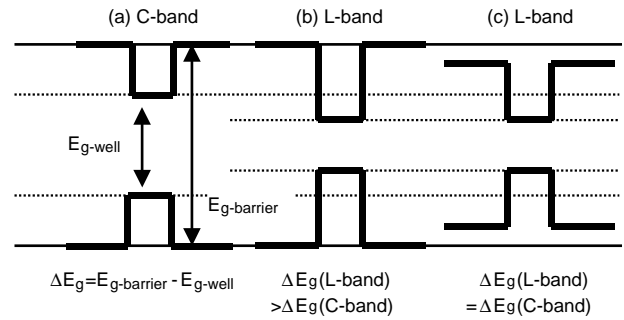


**Figure 5** Improvement of MQW structure in L-band.

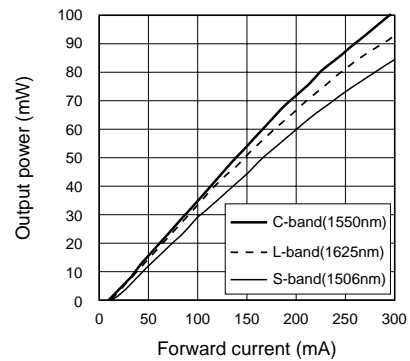


**Figure 6**  $L$ - $I$  curves among S-, L-band DFB LDs.

$\text{A/cm}^2$ ). The characteristic temperature  $T_0$ , which is calculated from the temperature dependence of  $I_{th}$ , is observed as the value of  $T_0 = 46 \text{ K}$ . This result shows that these LDs are very suitable for thermally tunable laser applications.

Figure 6 shows the  $L$ - $I$  curves of DFB LDs from S-band to L-band based on the previous discussion. As shown in this figure, the characteristic degradation in the L-band is not observed clearly and we achieved a very low driving current ( $< 200 \text{ mA}$ , @  $P_o=60 \text{ mW}$ ) in all wavelength regions. Comparing C and L-band, we observed a slightly higher driving current in the S-band, however, there is no problem in practical use. Finally, the median lifetime of these LDs is more than 73 years assuming a 20% increase in the driving current.

#### 5. NARROW SPECTRAL LINEWIDTH

In this section, we describe the approach used to get a narrow spectral linewidth for the key characteristic to extend our high power CW-DFB LDs to CATV applications. In CATV applications, the number of ports increases with output power, and an output power of over 80 mW is examined. To maintain a high S/N ratio even in analog propagation, a narrow linewidth of less than 1 MHz and a low RIN level of less than  $-160 \text{ dB/Hz}$  in 0~1 GHz are required. Generally the spectral linewidth seems to be inversely proportional to output power in low power region<sup>9)</sup>. However, there are many reports of the spectral linewidth

re-broadening in the high power region<sup>9), 10), 11)</sup>, and it is considered to be a very difficult problem to get a narrow linewidth in the high power region. The re-broadening is caused by the non-uniformity of the effective refractivity and the photon density in the cavity due to spatial hole burning (SHB). Non-uniformity of refractivity originates from the non-uniformity of carrier density due to the non-uniformity of photon density. On the other hand, the photon density distribution curve is determined by the facet phases, and these values cannot be controlled. To express photon density, the front to rear power ratio ( $P_f/P_r$ ) is considered to be a good parameter. In DFB LDs with symmetric facet coatings, linewidth re-broadening was suppressed by flattening the photon density in the phase shifted structure and multi-electrode<sup>12)</sup>. On the other hand, in the case of high power operation with asymmetric facet coatings, using a wide mesa is considered to be a very effective method to suppress re-broadening<sup>9)</sup>. Here, we achieved a very narrow linewidth by decreasing the carrier density in a long cavity and optimizing  $\kappa$  and  $P_f/P_r$  to get a highly uniform photon density. Figure 7 shows the spectral linewidth as a function of output power and cavity length. Here,  $\kappa L$  and  $P_f/P_r$  are fixed as 1.2 and 15, respectively, for the effects of SHB be suppressed as much as possible. We achieved the minimum linewidth of 0.5 MHz at 40 mW and 0.8 MHz, and even at 100 mW for a 800  $\mu\text{m}$  cavity. In addition, re-broadening is suppressed in a long cavity-

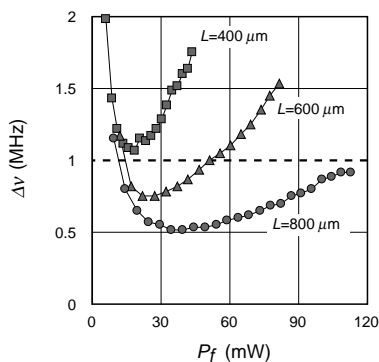


Figure 7 Spectral linewidth versus output power for LD with a cavity length of 400  $\mu\text{m}$ –800  $\mu\text{m}$

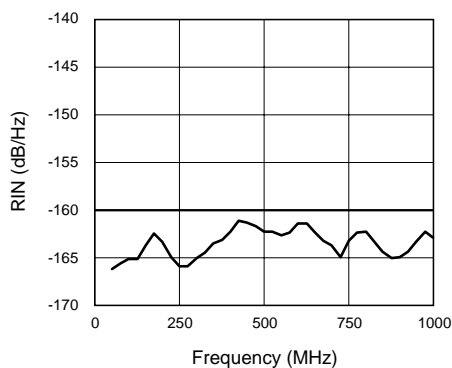


Figure 8 RIN data in 0~1 GHz. In all ranges, RIN<-160 dB/Hz was achieved.

ty. Thus, we demonstrated that a narrow linewidth in high power operation could be achieved by means of a long cavity and optimized  $\kappa L$  and  $P_f/P_r$ . Figure 8 shows RIN data. We also successfully achieved a very low RIN of -160 dB/Hz in 0~1 GHz. As a result, we achieved a very low noise characteristic that is sufficient to operate as a CATV signal source. Finally, we show the results of a reliability test in Figure 9. The figure shows that the increase of driving current as a function of aging hour in auto-power-control (APC) mode. We tested under an ambient temperature of 35°C and a chip output power of 120 mW constant (which is considered  $P_f>80$  mW). As shown, the increase of driving current is less than 1 % after 2000 hours of testing. These results show that the LD chips have a median lifetime of over 25 years and no problems in practical use.

## 6. CONCLUSION

Finally, we summarize this paper. We developed the high power CW-DFB LDs for optical communications. We took an approach to get low driving current from C-band to S and L-band for WDM systems. Considering optical and electronic confinement in optimizing the MQW structure, we achieved a very low driving current of less than 200 mA at a facet output power of 60 mW between S and L-band. To extend these LDs to CATV applications, we developed very high output power and low noise CW-DFB LDs. Concretely, using a long cavity and optimizing the coupling coefficient we achieved a high power of 175 mW and a very narrow linewidth of 0.8 MHz, even at 100 mW. These values are the highest values for commercial packages and these LDs have possible new applications in the future.

## ACKNOWLEDGEMENT

The authors would like to thank the members of Photonics & Packaging Technologies, Yokohama R & D Laboratories for their helpful support in all processes. They also would like to thank Fitel Optical Component Division for its helpful support in the packaging process.

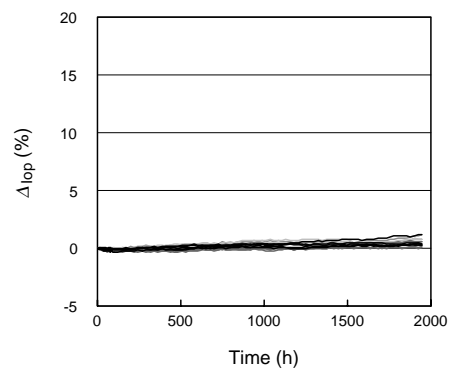


Figure 9 Changing rate of operating current under 35°C and 120 mW APC condition for 2000 hours.

## REFERENCES

- 1) T. Kise et al., "Over 100mW high power operation of 1625nm L-band DFB laser diodes", LEOS 2001, Technical Digest ThQ5, pp. 802-803, Nov. 2001.
- 2) H. Nasu et al., "40mW over DFB laser module with integrated wavelength monitor for 50GHz channel spacing DWDM application" ECOC 2001, Technical Digest We. P.25, pp.428-429, Oct. 2001
- 3) M. Funabashi et al., "Low Operating Current 40mW PM Fiber Coupled DFB Laser Modules for Externally Modulated 1550nm WDM Sources", ECOC Technical Digest Tu.B.1.3, pp. 122-123, 2001
- 4) J. D. Ralston et al., "High-Power fibre-coupled 1550nm DFB laser modules for externally-modulated fibre-optic transmission", Electron. Lett., 1997, 33, pp. 230-232
- 5) Y. Inaba et al., "High-Power 1.55- $\mu$ m Mass-Transport-Grating DFB Lasers for Externally modulated Systems", IEEE J. Select. Topics Quantum Electron., 2001, 7, pp.152-158
- 6) R. Menna et al., "High power 1550nm distributed feedback lasers with 440mW CW output power for telecommunication applications", CLEO Proc., 2001, CPD12-1-2
- 7) M. Funabashi et al., "High Power CW DFB Lasers and Modules for Externally Modulated WDM Sources", OECC 2002, Technical Digest 11C3-4, pp.478-479, July 2002
- 8) K. Takaki et al., "Spectral Linewidth Re-Broadening and Photon Density Distribution in 1550nm High Power CW-DFB Lasers", ISLC 2002, Technical Digest MC3, pp.23-24, Sep. 2002
- 9) C. H. Henry.: "Theory of the Linewidth of Semiconductor Lasers", IEEE J. Quantum Electron., 1982, 18, pp259-264
- 10) H. Wenzel et al., "Linewidth re-broadening in semiconductor lasers due to lateral spatial hole burning", Electron. Lett., vol. 27, pp. 2301-2302, 1991
- 11) X. Pan et al., "Spatial linewidth of DFB lasers including the effects of spatial hole burning and nonuniform current injection", IEEE Photon Technol. Lett., vol. 2, no. 8, pp.312-315, 1990
- 12) M. Okai et al., "Corrugation-Pitch-Modulated MQW-DFB Laser with Narrow Spectral Linewidth (170kHz)", IEEE Photon Technol. Lett., vol. 2, no. 8, pp.529-530, 1990